JACS
JOURNAL OF THE AMERICAN CHEMICAL SOCIETY
pubs.acs.org/JACS
Article

Fluoroarene Separations in Metal−Organic Frameworks with Two Proximal Mg^{2+} Coordination Sites

Mary E. Zick, Jung-Hoon Lee, Miguel I. Gonzalez, Ever O. Velasquez, Adam A. Uliana, Jaehwan Kim, Jeffrey R. Long, and Phillip J. Milner*

Cite This: J. Am. Chem. Soc. 2021, 143, 1948−1958
Read Online

ABSTRACT: Fluoroarenes are widely used in medicinal, agricultural, and materials chemistry, and yet their production remains a critical challenge in organic synthesis. Indeed, the nearly identical physical properties of these vital building blocks hinders their purification by traditional methods, such as flash chromatography or distillation. As a result, the Balz−Schiemann reaction is currently employed to prepare fluoroarenes instead of more atom-economical C−H fluorination reactions, which produce inseparable mixtures of regioisomers. Herein, we propose an alternative solution to this problem: the purification of mixtures of fluoroarenes using metal−organic frameworks (MOFs). Specifically, we demonstrate that controlling the interaction of fluoroarenes with adjacent coordinatively unsaturated Mg^{2+} centers within a MOF enables the separation of fluoroarene mixtures with unparalleled selectivities. Liquid-phase multicomponent equilibrium adsorption data and breakthrough measurements coupled with van der Waals-corrected density functional theory calculations reveal that the materials Mg_2(dobdc) (dobdc^{4-} = 2,5-dioxidobenzene-1,4-dicarboxylate) and Mg_2(*m*-dobdc) (*m*-dobdc^{4-} = 2,4-dioxidobenzene-1,5-dicarboxylate) are capable of separating the difluorobenzene isomers from one another. Additionally, these frameworks facilitate the separations of fluoroanisoles, fluorotoluenes, and fluorochlorobenzenes. In addition to enabling currently unfeasible separations for the production of fluoroarenes, our results suggest that carefully controlling the interaction of isomers with not one but two strong binding sites within a MOF provides a general strategy for achieving challenging liquid-phase separations.

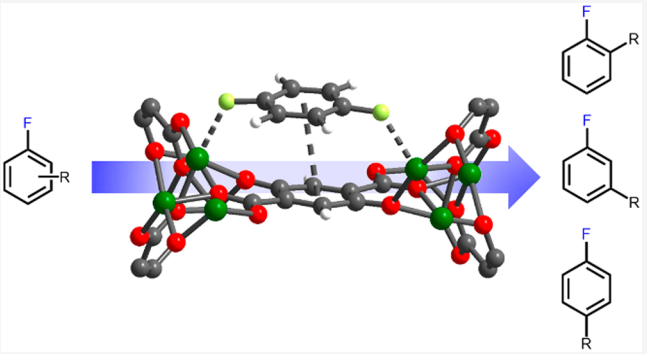

INTRODUCTION

Fluorinated compounds such as fluoroarenes are ubiquitous in the pharmaceutical[1−4] and agrochemical[5] industries because fluorination generally improves the bioavailability, lipophilicity, and metabolic stability of target molecules. Indeed, approximately 20% of pharmaceuticals and 30% of agrochemicals are fluorinated.[3,5] In addition, fluorinated building blocks are critical for the production of fluoropolymers such as Teflon.[6] Despite decades of method development, the synthesis of fluorinated compounds still generally requires pre-functionalized starting materials and harsh reaction conditions.[7−11] For example, the most widely used industrial method to prepare simple fluoroarenes is the Balz−Schiemann reaction, which involves the thermolysis of aryl tetrafluoroborate diazonium salts (Figure 1a, left).[12] This reaction generally results in low yields, presents significant safety hazards due to the explosiveness of diazonium salts, and requires an aniline starting material, which is typically prepared from the corresponding arene.[13] In contrast, the most sustainable and atom-economical strategy to prepare fluoroarenes would be via the undirected C−H fluorination of arenes using fluorine (F_2) or transition-metal-catalyzed methods (Figure 1a, right).[8,14−16] However, C−H fluorination often produces mixtures of fluoroarene regioisomers (Ar−F) along with residual starting arene (Ar−H),[14−16] all of which are nearly impossible to separate from one another using chromatography or distillation.[16−20] Therefore, the development of new strategies for the selective purification of mixtures of fluoroarene regioisomers, as well as fluoroarenes from the corresponding arenes, would enable currently unrealized and potentially more atom-economical strategies for the production of fluoroarenes on industrial scale (Figure 1b).

Metal−organic frameworks (MOFs) are porous, crystalline solids, composed of metal nodes and organic linkers, that exhibit a high degree of chemical and structural diversity.[21] These features have positioned MOFs as promising candidate solid

Received: November 2, 2020
Published: January 25, 2021

https://dx.doi.org/10.1021/jacs.0c11530
J. Am. Chem. Soc. 2021, 143, 1948−1958

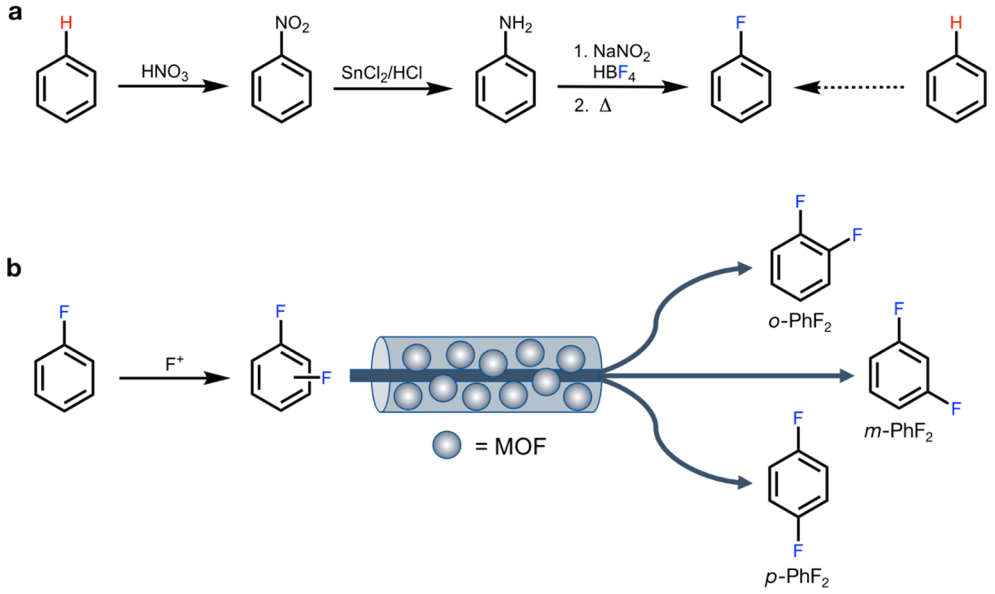

Figure 1. A nitration−reduction−diazotization route (a) is generally used to prepare fluoroarenes because the more facile electrophilic C−H fluorination of arenes is not selective, and the separation of the resulting isomers remains a significant challenge. (b) The discovery of a suitable adsorbent capable of effective fluoroarene isomer separation would enable the use of C−H fluorination for the synthesis of valuable fluorinated arenes (this work).

phases for chromatographic separations,[22−29] although this application remains vastly underexplored compared to the development of such materials for gas separations.[30,31] Similar to molecular sieves and thin-film membranes, MOFs have been studied for shape- and size-based kinetic separations in the liquid phase.[32−39] Additionally, MOFs have been shown to separate adsorbates on the basis of selective interactions with specific functional groups,[34,36−48] enabling separations based on the differential interaction of guest molecules with strong binding sites.[49−53] However, size-selective separations of fluoroarene isomers are not viable because fluorine is nearly the same size as hydrogen, and organofluorines only weakly engage in intermolecular interactions such as hydrogen- or halogen-bonding, limiting the strength of adsorbate−adsorbent interactions.[35] Hence, a distinct strategy is required to harness MOFs as a platform for the challenging separation of fluoroarene isomers.

Effective separations of small molecules (e.g., CO_2 from N_2) using MOFs are generally predicated on the selective interaction of adsorbates with a single, well-defined binding site, such as a coordinatively unsaturated metal center.[31,54] Because fluoroarenes should interact weakly with open metal centers,[55−58] we hypothesized that carefully tuning the interaction of fluoroarenes with *multiple* open metal centers in a framework would lead to higher selectivities than can be achieved at a single site. Indeed, recent work has shown that the framework Co_2(dobdc) (dobdc^{4-} = 2,5-dioxidobenzene-1,4-dicarboxylate) is able to efficiently separate the C_8 alkylaromatics *o*-xylene, *m*-xylene, *p*-xylene, and ethylbenzene as a result of the unique synergistic interactions of two adjacent open cobalt(II) sites with each isomer.[59] Herein, we demonstrate that a similar strategy enables the general purification of mixtures of fluoroarene regioisomers, as well as mixtures of arenes based on the degree of fluorination. Thus, tuning the interactions of liquid adsorbates with multiple strong, well-defined binding sites can provide a powerful and general means for achieving otherwise challenging chromatographic separations.

RESULTS AND DISCUSSION

Separation of Difluorobenzene Isomers. The separation of *o*-difluorobenzene (*o*-PhF_2), *m*-difluorobenzene (*m*-PhF_2), and *p*-difluorobenzene (*p*-PhF_2) is one example of the challenging purification of fluoroarene regioisomers (Figure 1). These difluorobenzenes are valuable building blocks in the pharmaceutical industry, and *o*-PhF_2 is a widely used (and costly) solvent.[60] Notably, the direct fluorination of fluorobenzene (PhF) with F_2 produces a mixture of all three compounds that is challenging to purify using conventional methods.[61] To the best of our knowledge, this difficult separation has never been explored using MOFs, leading us to select it as an initial target for our proposed strategy.

Exploring the purification of difluorobenzenes via controlled interactions with multiple adjacent metal centers requires frameworks with high densities of open metal sites spaced approximately 6−8 Å apart, or slightly longer than the length of *p*-PhF_2 (∼5.5 Å). The M_2(dobdc) (M = Mg, Mn, Fe, Co, Ni, Cu, Zn, Cd) or M-MOF-74[62−64] family of frameworks was therefore identified as a promising target, given that it features coordinatively unsaturated metal cations spaced approximately 8 Å apart along one-dimensional hexagonal channels.[59] We also chose to investigate the isomeric family M_2(*m*-dobdc) (M = Mg, Mn, Fe, Co, Ni; *m*-dobdc^{4-} = 2,4-dioxidobenzene-1,5-dicarboxylate), which bears open metal sites that are more Lewis acidic and spaced slightly more closely than those in M_2(dobdc) (Figure 2b).[65] The range of cations that can be incorporated into both structures further offers an opportunity to interrogate subtle differences in framework geometry and F···M interaction strength on the binding of difluorobenzenes. In addition, we sought to explore the isoreticularly expanded analogue of M_2(dobdc), namely M_2(dobpdc) (M = Mg, Mn, Fe, Co, Ni, Zn; dobpdc^{4-} = 4,4′-dioxidobiphenyl-3,3′-dicarboxylate), which possesses a similar overall topology but with metal centers spaced 10−12 Å apart (Figure 2c).[66−68] Finally, the well-studied framework Cu_3(btc)$_2$ (btc^{3-} = 1,3,5-benzenetricarboxylate) or HKUST-1 also features accessible metal sites spaced

https://dx.doi.org/10.1021/jacs.0c11530
J. Am. Chem. Soc. 2021, 143, 1948−1958

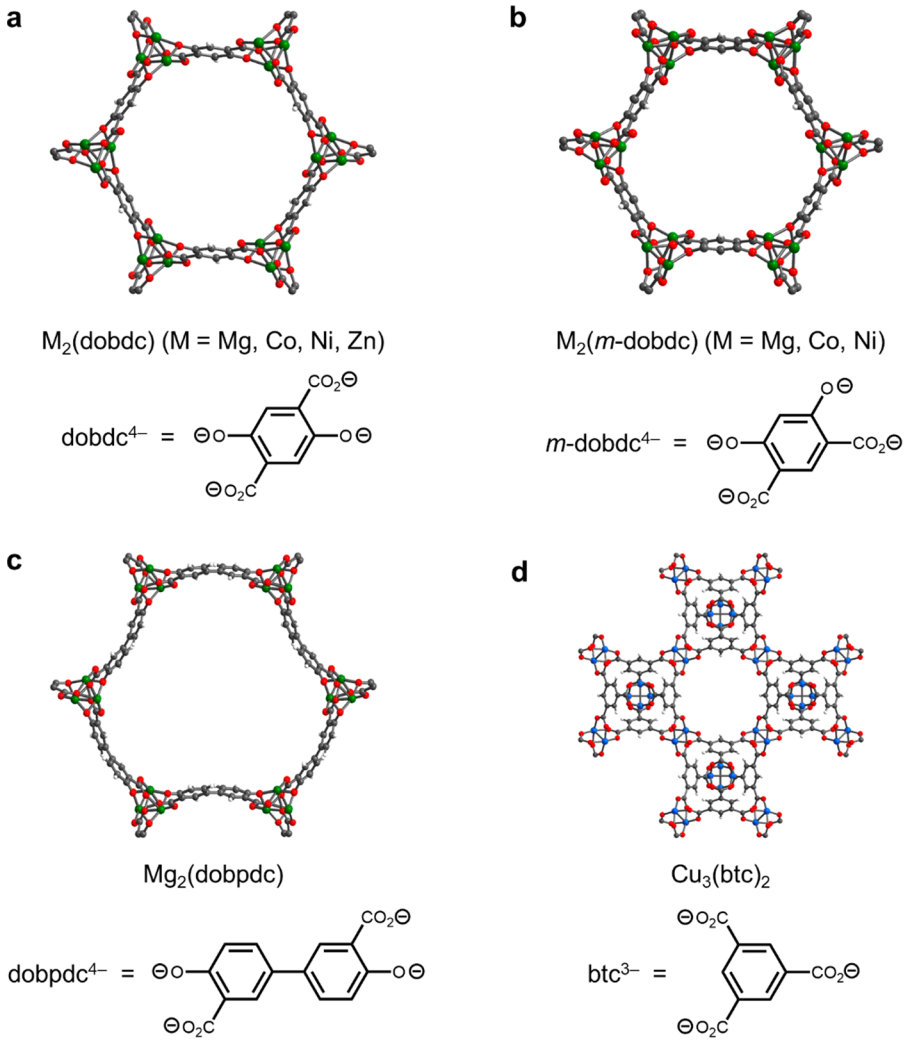

Figure 2. Metal−organic frameworks bearing coordinatively unsaturated metal centers studied in this work for the separation of fluoroarene regioisomers. (a) M_2(dobdc) (M = Mg, Co, Ni, Zn), (b) M_2(*m*-dobdc) (M = Mg, Co, Ni), (c) Mg_2(dobpdc), and (d) $Cu_3(btc)_2$. Gray, white, green, red, and blue spheres correspond to carbon, hydrogen, magnesium, oxygen, and copper, respectively.

approximately 8 Å apart and was therefore selected as an alternative candidate solid phase (Figure 2d).[69] Literature procedures for the synthesis of M_2(dobdc) (M = Mg, Co, Ni, Zn), M_2(*m*-dobdc) (M = Mg, Co, Ni), Mg_2(dobpdc), and $Cu_3(btc)_2$ were adapted to prepare these materials on scales of greater than 1 g. Following synthesis, the compounds were thoroughly solvent-exchanged, and their purity and crystallinity were confirmed by comparing their powder X-ray diffraction patterns and 77 K N_2 surface areas to those reported in the literature (see Section 3 of the Supporting Information (SI) for details). As a control, we also analyzed the fluoroarene adsorption properties of CD-MOF-1 (CD = γ-cyclodextrin), which is prepared from inexpensive, edible ingredients and has previously been shown to separate mixtures of haloarenes (e.g., PhF from PhCl) (see Section 5 of the SI for details).[49,70]

Isothermal multicomponent liquid-phase adsorption measurements were first carried out to assess the ability of the frameworks bearing open metal sites to partition a mixture of *o*-, *m*-, and *p*-PhF_2. These competitive adsorption experiments provide insight into the performance of MOFs under mixed-adsorbate conditions, which can differ dramatically from the ideal selectivities predicted from single-component measurements. Briefly, in an N_2-filled glovebox, 4 mL vials containing fully desolvated samples of each MOF (in triplicate) were charged with an equimolar (~0.5 M) mixture of *o*-, *m*-, and *p*-PhF_2 in heptanes. The vials were left to stand for 24 h, after which time the supernatants were analyzed by ^{19}F NMR and compared to the initial solution, enabling the independent quantification of each fluoroarene adsorbed within each framework (see the Section 2 of the SI). In addition to this indirect measurement of fluoroarene adsorption, fluoroarene binding in Mg_2(dobdc) was also confirmed directly by magic angle spinning solid-state ^{19}F NMR and transmission IR measurements (see Section 9 of the SI for details). From the multicomponent uptake data, competitive selectivities, S, for component i over component j were calculated using eq 1, in which q_i and q_j are the amount of each component adsorbed at equilibrium (in mmol/g) and c_i and c_j are the concentrations of each component at equilibrium (in M).

$$S = \frac{q_i/q_j}{c_i/c_j} \tag{1}$$

In general, the adsorption affinity for all frameworks follows the trend *p*-PhF_2 > *m*-PhF_2 > *o*-PhF_2 (Figure 3), and by far the highest selectivities were measured for the Mg-based frame-

https://dx.doi.org/10.1021/jacs.0c11530
J. Am. Chem. Soc. 2021, 143, 1948−1958

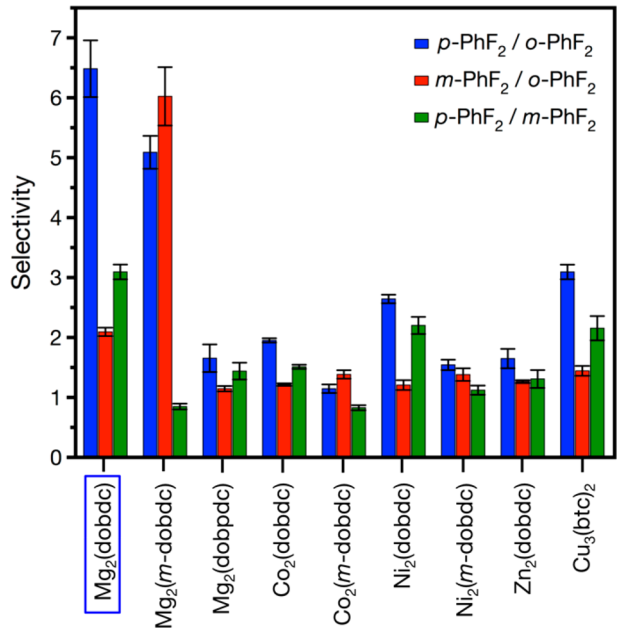

Figure 3. Summary of adsorption selectivities calculated from isothermal equilibrium three-component data for uptake of *o*-, *m*-, and *p*-difluorobenzene in various MOFs. Each value represents the average of three separate measurements. Samples were dosed with an approximately equimolar mixture (~0.5 M in each isomer) in heptanes and allowed to equilibrate at room temperature over 24 h followed by analysis of the supernatant by ^{19}F NMR.

works Mg_2(dobdc) and Mg_2(*m*-dobdc) (SI, Table S1). Among all studied frameworks, Mg_2(dobdc) was uniquely able to partition the difluorobenzenes mixture, with high selectivities of 6.5 ± 0.5, 3.1 ± 0.1, and 2.1 ± 0.1 for *p*-PhF_2/*o*-PhF_2, *p*-PhF_2/*m*-PhF_2, and *m*-PhF_2/*o*-PhF_2, respectively (SI, Table S1). These data were independently verified by two-component adsorption measurements, which yielded similar or higher selectivities in all cases (see Section 6 of the SI for details). On the other hand, while Mg_2(*m*-dobdc) demonstrated very high selectivities for both *p*-PhF_2 and *m*-PhF_2 over *o*-PhF_2, it was unable to discriminate between *m*-PhF_2 and *p*-PhF_2 (see below). The superior performance of these two frameworks is ascribed in part to the hardness of the exposed Mg^{2+} cations, which should engage in stronger interactions with the similarly hard F atoms of the difluorobenzene isomers than Ni^{2+}, Cu^{2+}, Co^{2+}, or Zn^{2+} sites.[55−58] Indeed, the calculated hardness parameter (η_A) of Mg^{2+} is significantly larger (32.5 eV) than for Ni^{2+} (8.5 eV), Cu^{2+} (8.3 eV), and Zn^{2+} (10.8 eV).[71] Additionally, there are several reports of crystallographically characterized molecular complexes featuring fluoroarenes engaged in short Mg^{2+}···F contacts.[72,73] Finally, the comparatively poor performance of Mg_2(dobpdc) for separating difluorobenzenes indicates that, in addition to a high-density of hard Mg^{2+} centers, the distance between metal ions is a critical factor influencing selectivity. Overall, these results demonstrate that frameworks bearing a high density of closely spaced Mg^{2+} centers are capable of differentiating between difluorobenzene isomers.

Van der Waals (vdW)-corrected density functional theory (DFT) calculations were carried out to probe the binding mode of each difluorobenzene isomer within Mg_2(dobdc) (see Section 10 of the SI for details). A comparison of the lowest-energy structures of the difluorobenzene isomers in Mg_2(dobdc) reveals that all three isomers display off-centered $\pi-\pi$ stacking interactions with the benzene ring of a $dobdc^{4-}$ linker, with centroid-to-centroid distances of 3.71, 3.60, and 3.24 Å for *o*-PhF_2, *m*-PhF_2, and *p*-PhF_2, respectively (Figure 4). The shorter distance for *p*-PhF_2 reflects the superior packing of this adsorbate in the pores compared to the other two isomers. Of note, these calculated $\pi-\pi$ distances are similar to those previously reported for xylene isomers adsorbed in Co_2(dobdc) (3.58−3.65 Å).[59] In addition, all three difluorobenzene isomers are predicted to bridge two adjacent metal sites on opposing sides of a $dobdc^{4-}$ linker via at least one Mg···F interaction.[55−58] Whereas *o*-PhF_2 and *m*-PhF_2 bind to these sites via one Mg···F and one weak Mg···H−C interaction, the 1,4-substitution of *p*-PhF_2 allows both fluorine atoms to strongly interact with both metal centers, with calculated Mg···F distances of 2.39 and 2.43 Å. The unique bridging mode available to *p*-PhF_2 within Mg_2(dobdc) likely accounts for its selective binding over the other two isomers (Figure 3). The preferred binding of *m*-PhF_2 over *o*-PhF_2 can be ascribed to the stronger inductive electron-withdrawing effect of the non-binding fluorine atom in *o*-PhF_2, which leads to a longer predicted Mg···F distance for *o*-PhF_2 (2.90 Å) than for *m*-PhF_2 (2.46 Å). Finally, the magnitudes of the calculated adsorption energies (ΔE_{ads}) decrease from *p*-PhF_2 to *m*-PhF_2 to *o*-PhF_2, consistent with the experimental selectivity results. Calculated structures for difluorobenzene binding in Mg_2(*m*-dobdc) also support the selectivity trends observed for this material (SI, Figures S66 and S67). Specifically, the slightly closer spacing of Mg^{2+} centers in Mg_2(*m*-dobdc) allows *m*-PhF_2

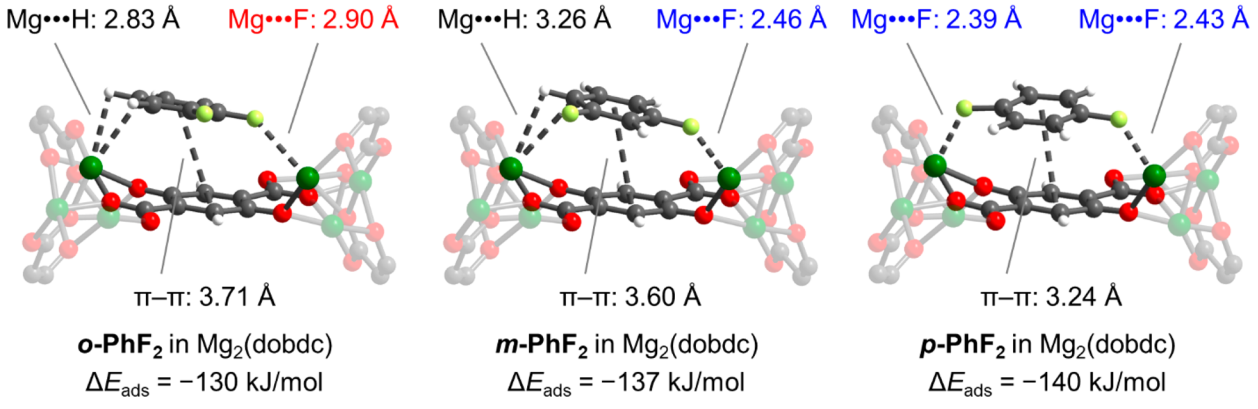

Figure 4. Density functional theory structures for *o*-PhF_2 (left), *m*-PhF_2 (center), and *p*-PhF_2 (right) adsorbed in Mg_2(dobdc). Gray, white, dark green, yellow-green, and red spheres correspond to carbon, hydrogen, magnesium, fluorine, and oxygen atoms, respectively.

https://dx.doi.org/10.1021/jacs.0c11530
J. Am. Chem. Soc. 2021, 143, 1948−1958

to bridge two metal centers in a manner similar to *p*-PhF_2, leading to a lack of selectivity between these isomers (Figure 3). Overall, these calculations suggest that a combination of inductive effects and bridging interactions between adjacent Mg^{2+} centers account for the unique ability of Mg_2(dobdc) to enable the difficult separation of difluorobenzene isomers.

Single-crystal X-ray diffraction data can provide valuable confirmation of predicted adsorbate binding in porous frameworks, although it is challenging to grow sufficiently large crystals of Mg_2(dobdc) for *in situ* X-ray diffraction experiments. As such, single-crystal X-ray diffraction data were instead obtained for samples of Co_2(dobdc) loaded with *p*-, *m*-, and *o*-PhF_2 to corroborate the predicted structures for these difluorobenzenes within Mg_2(dobdc) (see Section 12 of the SI for details), as our preliminary vdW-corrected DFT calculations indicate that *p*-, *m*-, and *o*-PhF_2 are predicted to favor the same binding modes in Co_2(dobdc) as in Mg_2(dobdc) (SI, Figure S69).[59,74] Specifically, twinned single crystals of Co_2(dobdc) were desolvated under vacuum at 180 °C and then soaked in pure, anhydrous fluoroarene under an inert atmosphere for at least 4 h before analysis by X-ray diffraction at 100 K. However, *m*-PhF_2 and *o*-PhF_2 bound within Co_2(dobdc) were too disordered to yield meaningful structural information, and the orientation of the guest molecules could not be resolved. Therefore, fluorobenzene (PhF) was chosen as a proxy, as this molecule should bridge two metal centers in a manner similar to that predicted for *m*-PhF_2 and *o*-PhF_2. Consistently, computational analysis suggests that PhF favors such a bridging mode within Mg_2(dobdc) (SI, Figure S68), and competitive equilibrium adsorption measurements of PhF and *p*-PhF_2 in Mg_2(dobdc) indicate that PhF binds more weakly within this material (SI, Figure S43).

Analysis of the single-crystal X-ray diffraction data for *p*-PhF_2 in Co_2(dobdc) revealed a structure with the formula Co_2(dobdc)·1.30(*p*-PhF_2), wherein the primary adsorption site for *p*-PhF_2 (45.0(5)% occupancy) is similar to that predicted for *p*-PhF_2 in Mg_2(dobdc) (Figure 5, upper).

In particular, the fluoroarene molecule bridges two adjacent cobalt centers with equal Co···F distances of 2.469(19) Å. These distances are similar to the calculated Mg···F distances (2.39–2.43 Å), albeit slightly longer due to the expected weaker nature of the Co···F interaction. The π–π distance of 3.249(8) Å in the Co_2(dobdc) structure also compares well with the calculated distance of 3.24 Å in the Mg_2(dobdc) structure. In the case of PhF-loaded crystals of Co_2(dobdc), refinement of the diffraction data revealed a structure with the formula Co_2(dobdc)·1.20(*p*-PhF), wherein PhF preferentially bridges two adjacent metal centers (47.5(10)% occupancy) via Co···F (2.63(3) Å) and Co···H–C (Co–C distance of 3.019(14) Å) interactions (Figure 5, lower). As hypothesized, this coordination mode is similar to the calculated structures for *o*- and *m*-PhF_2 adsorbed within Mg_2(dobdc) (Figure 4). All together, these data support the proposed origin of selectivity for adsorption of *p*-PhF_2 in Mg_2(dobdc) over *m*-PhF_2 and *o*-PhF_2 as arising from multiple strong metal–adsorbate interactions. We note that additional binding sites were located for *p*-PhF_2 and PhF in Co_2(dobdc) involving interactions with only a single cobalt site, with Co···F distances of 2.347(16) and 2.255(16)–2.399(15) Å, respectively (SI, Figures S80 and S81). As the framework becomes saturated with fluoroarene molecules, adsorbate–adsorbate interactions are expected to become available to stabilize these adsorption sites with only a single Co···F interaction, making them competitive with those that possess two Co···F interactions.

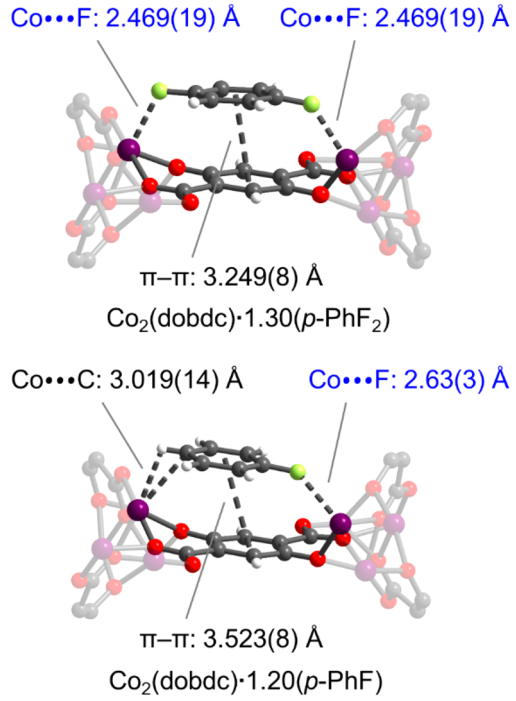

Figure 5. Single-crystal X-ray diffraction structures of *p*-PhF_2 (upper) and PhF (lower) in Co_2(dobdc) obtained at 100 K with key framework–adsorbate interactions indicated. Gray, white, purple, yellow-green, and red spheres correspond to carbon, hydrogen, cobalt, fluorine, and oxygen atoms, respectively.

Notably, crystallographic characterization of complexes that feature a fluoroarene interacting with a transition metal through the fluorine atom remain relatively rare and are largely limited to early transition metals,[55–58,75–79] although such motifs are presumably intermediates in C–F bond activation processes.[80–82] In particular, while there are several crystallographically characterized complexes in which fluoroarenes interact with a cobalt center through the π-system,[83–88] to the best of our knowledge there is only one other reported structure containing a Co···F interaction (2.65(2) Å).[79] Therefore, in addition to corroborating the presumptive modes of fluoroarene binding in Mg_2(dobdc), these structures represent rare examples of fluoroarenes coordinated to a Lewis acidic transition metal center through fluorine.

Based on the preceding structural analysis, the primary *p*-PhF_2 binding site in Mg_2(dobdc) should saturate at a loading of approximately one molecule per two Mg^{2+} sites (4.1 mmol/g). To verify this capacity experimentally, we carried out multicomponent liquid-phase adsorption measurements over a range of initial fluoroarene concentrations up to a maximum of 2.0 M in heptanes (Figure 6), approaching the concentration of a neat mixture of difluorobenzenes (approximately 3.3 M at 25 °C). Consistent with the expected bridging mode, the adsorption capacity of *p*-PhF_2 was found to saturate at approximately 4.0 mmol/g for *p*-PhF_2 concentrations above 1.0 M. In addition, over the entire concentration range, isomer uptake in Mg_2(dobdc) followed the trend *p*-PhF_2 > *m*-PhF_2 > *o*-PhF_2. At a concentration of approximately 1.5 M, the total difluorobenzene uptake was found to be approximately 6.3 mmol/g (77% metal site occupancy), suggesting that there is a mixture of isomers interacting with one and two metal centers at higher

https://dx.doi.org/10.1021/jacs.0c11530
J. Am. Chem. Soc. 2021, 143, 1948–1958

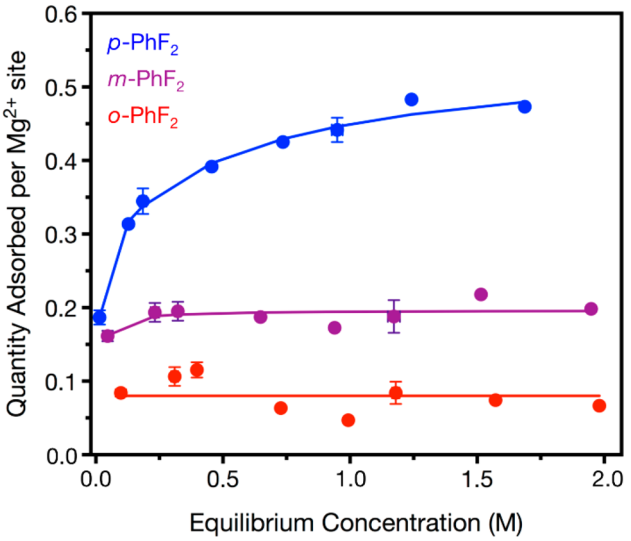

Figure 6. Isothermal equilibrium three-component adsorption data for uptake of *o*-, *m*-, and *p*-PhF_2 in Mg_2(dobdc) starting from various initial equimolar concentrations (in heptanes). The samples were dosed with an approximately equimolar mixture and allowed to equilibrate at room temperature over 24 h before the equilibrium concentration of each fluoroarene was determined by ^{19}F NMR (in comparison to an internal standard).

concentrations (SI, Figures S80 and S81). Nonetheless, these data confirm that the synergistic interaction of *p*-PhF_2 with adjacent metal sites in Mg_2(dobdc) leads to selective adsorption of this isomer at a range of concentrations.

Multicomponent liquid-phase breakthrough measurements were next carried out to evaluate the difluorobenzene separation performance of Mg_2(dobdc) under dynamic conditions (Figure 7; see Section 11 of the SI for details). Typically, breakthrough

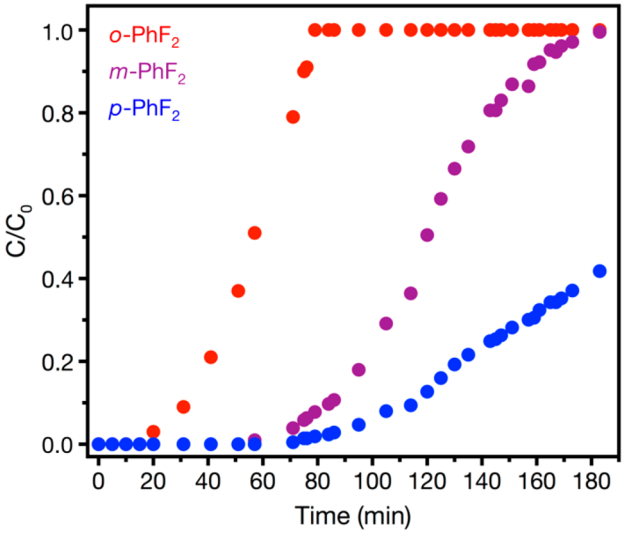

Figure 7. Multicomponent liquid-phase breakthrough measurement for an equimolar mixture ($C_0 \approx 33$ mM in hexanes) of *o*-, *m*-, and *p*-PhF_2 in Mg_2(dobdc) at room temperature. Concentrations were determined by ^{19}F NMR in comparison to an internal standard until *o*-PhF_2 reached saturation at a time of 79 min. After this point, the *o*-PhF_2 concentration was assumed to be constant, and concentrations for *m*- and *p*-PhF_2 were determined in comparison to the measured *o*-PhF_2 saturation concentration to avoid error introduced from the addition of the internal standard.

measurements using liquid adsorbates are either carried out in the vapor phase, to mimic gas-phase measurements, or using a liquid chromatography instrument with the adsorbent as the solid phase.[22−29,49,59] However, both of these measurements have drawbacks: vapor-phase measurements may not reflect the selectivities, capacities, or kinetics observed in the liquid phase, whereas liquid chromatography measurements require expensive instrumentation that is not readily translated to an inert atmosphere, such as an N_2-filled glovebox. To overcome these limitations, we constructed an inexpensive breakthrough apparatus consisting of a narrow glass column connected to a syringe pump, which can be utilized on the benchtop or inside of an inert atmosphere glovebox (SI, Figure S70). For the experiments described here, the column was charged with approximately 1.10 g of roughly pelletized and fully activated Mg_2(dobdc) (350−700 μm diameter spherical particles) in a N_2-filled glovebox (SI, Figures S70−S73). After flushing the column with anhydrous hexanes, an equimolar mixture of *o*-, *m*-, and *p*-PhF_2 (33 mM in hexanes) was introduced at a controlled rate using the syringe pump. The outlet feed was collected in 0.5 mL increments and analyzed by ^{19}F NMR spectroscopy against an internal standard to determine the concentration of each difluorobenzene.

Consistent with multicomponent equilibrium adsorption measurements, *o*-PhF_2 eluted first, followed by *m*-PhF_2 and finally *p*-PhF_2, the strongest-binding isomer (Figure 7). The difluorobenzene isomers should possess similar diffusivities within the pores of Mg_2(dobdc) due to their nearly identical sizes and shapes; as such, this separation is likely dominated by the observed thermodynamic selectivities. Consistently, preliminary breakthrough measurements with Ni_2(*m*-dobdc), which displays poor selectivities under equilibrium conditions (Figure 3), confirmed that this MOF is incapable of separating a mixture of difluorobenzene isomers under dynamic conditions as well (SI, Figure S77). Adsorption capacities for *o*-PhF_2 and *m*-PhF_2 were calculated by integrating the breakthrough curves and found to be 0.83 and 2.04 mmol/g, respectively. Because *p*-PhF_2 did not completely elute by the end of the experiment, the *p*-PhF_2 breakthrough curve was extrapolated to saturation using the slope between 105 and 183 min and the total area under the resulting curve was integrated to yield a value of 3.54 mmol/g. Using the calculated capacities and the measured initial concentrations of each difluorobenzene in the feed solution (30.1, 34.0, and 35.1 mM for *o*-, *m*-, and *p*-PhF_2, respectively), calculated selectivities of 3.67, 2.19, and 1.68 were determined for *p*-PhF_2/*o*-PhF_2, *m*-PhF_2/*o*-PhF_2, and *p*-PhF_2/*m*-PhF_2, respectively (eq 1). The breakthrough selectivity for *m*-PhF_2/*o*-PhF_2 is consistent with the equilibrium batch selectivity (2.1 ± 0.1), but the *p*-PhF_2/*o*-PhF_2 and *p*-PhF_2/*m*-PhF_2 breakthrough selectivities are slightly lower than those determined from multicomponent equilibrium batch experiments (6.5 ± 0.5 and 3.1 ± 0.1, respectively). These minor differences suggest that competitive effects in a transient system affect the multicomponent adsorption behavior. Nonetheless, the breakthrough data confirm that Mg_2(dobdc) is able to partition the three difluorobenzenes in real time. In addition, Mg_2(dobdc) was found to retain its crystallinity and porosity after the breakthrough measurement (SI, Figures S74 and S75). Importantly, the successful performance of Mg_2(dobdc) in these breakthrough measurements also confirms that a rapid, small-scale multicomponent equilibrium assay is sufficient to forecast the utility of a given framework for a fixed-bed liquid-phase separation.

https://dx.doi.org/10.1021/jacs.0c11530
J. Am. Chem. Soc. 2021, 143, 1948−1958

Separations of Other Fluoroarene Mixtures. Having demonstrated the exceptional ability of Mg_2(dobdc) to separate difluorobenzene regioisomers, we sought to evaluate the scope of fluoroarene separations that can be accomplished using this framework. A major challenge for electrophilic C−H fluorination is that the Ar−F products are difficult to separate from the starting Ar−H using standard chromatographic methods.[16,17,19,20] The separations of these mixtures by distillation is also challenging; for example, the boiling point of fluorobenzene (85 °C) is similar to that of all three difluorobenzene isomers (82−92 °C). However, our crystallographic and computational analyses suggest that it may be possible to separate PhF from the difluorobenzene isomers due to the distinct interactions that this molecule exhibits with adjacent metals centers in Mg_2(dobdc).

The ability of Mg_2(dobdc) to separate fluoroarenes based on the degree of fluorination was evaluated by performing equilibrium two-component (PhF and PhF_2) and four-component (PhF, *o*-, *m*-, and *p*-PhF_2) adsorption experiments involving fluorobenzene and the difluorobenzene regioisomers (see Section 7 of the SI). The selectivities resulting from the two-component measurements are summarized in Figure 8. As

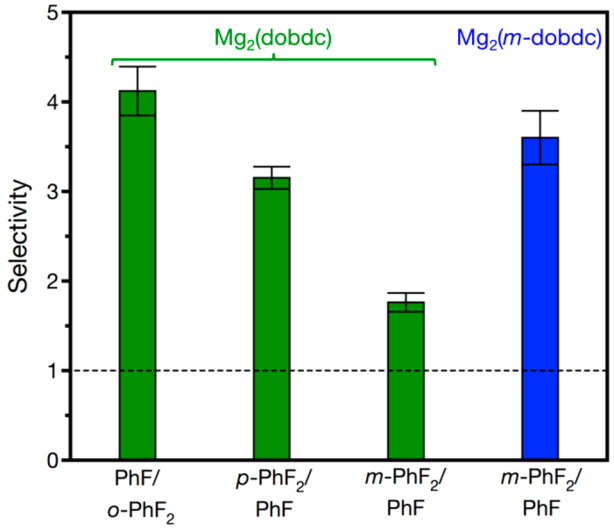

Figure 8. Summary of isothermal equilibrium two-component adsorption selectivities of Mg_2(dobdc) for PhF/*o*-PhF_2, *p*-PhF_2/PhF, and *m*-PhF_2/PhF (green) and of Mg_2(*m*-dobdc) for *m*-PhF_2/PhF (blue). Samples were dosed with an approximately equimolar mixture (~0.5 M in each isomer) in heptanes and allowed to equilibrate at room temperature over 24 h followed by analysis of the supernatant by ^{19}F NMR. Each value represents the average of three separate measurements. A line corresponding to a selectivity of 1 (i.e., not selective) is included for reference.

already discussed above, Mg_2(dobdc) preferentially binds *p*-PhF_2 over PhF with a selectivity of 3.2 ± 0.1, due to the unique ability of *p*-PhF_2 to bridge two metal centers via M···F interactions (SI, Figure S43). Interestingly, Mg_2(dobdc) was found to preferentially bind PhF over *o*-PhF_2 with a selectivity of 4.1 ± 0.3 (SI, Figure S44), likely a result of stronger Mg···F interactions with PhF. Finally, Mg_2(dobdc) exhibits only a slight preference (1.8 ± 0.1) for adsorption of *m*-PhF_2 over PhF (SI, Figure S45), an unsurprising result given that these two fluoroarenes are both expected to bind to two adjacent metal centers via one Mg···F interaction and one Mg···H−C interaction. Indeed, Mg_2(dobdc) was unable to partition PhF and *m*-PhF_2 effectively in the four-component adsorption experiment (SI, Figure S42). However, the framework is capable of effecting the challenging separation of PhF from both *o*-PhF_2 and *p*-PhF_2 in a mixture of all four fluoroarenes.

In principle, a higher *m*-PhF_2/PhF selectivity should be possible using a framework in which *m*-PhF_2 is able to bridge neighboring metal centers via Mg···F interactions. As discussed above, our vdW-corrected DFT calculations indicate that *m*-PhF_2 uniquely adopts this bridging mode in Mg_2(*m*-dobdc) due to the closer spacing of Mg centers in this framework, whereas PhF binds in the material via Mg···F and Mg···H−C interactions (Figure 9). As a result, the predicted binding energy for *m*-PhF_2

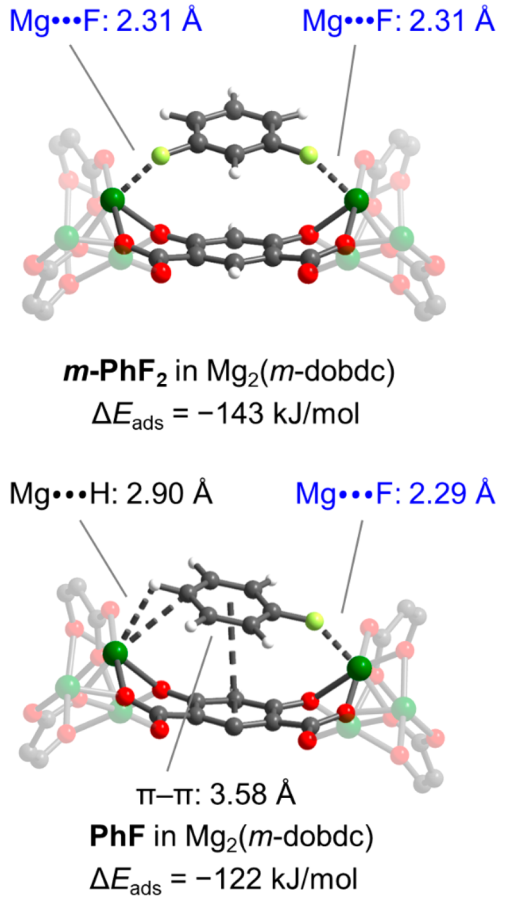

Figure 9. Density functional theory structures for binding of *m*-PhF_2 (upper) and PhF (lower) in Mg_2(*m*-dobdc). Gray, white, dark green, yellow-green, and red spheres correspond to carbon, hydrogen, magnesium, fluorine, and oxygen atoms, respectively.

is larger in magnitude than for PhF in Mg_2(*m*-dobdc). Gratifyingly, Mg_2(*m*-dobdc) indeed exhibits enhanced selectivity for binding *m*-PhF_2 over PhF (Figure 8) that is unparalleled among the MOFs studied here (SI, Figure S46). Based on these results, it should be possible to separate an equimolar mixture of PhF and the three PhF_2 regioisomers by first passing the mixture through Mg_2(dobdc) to generate streams of pure *o*-PhF_2, pure *p*-PhF_2, and a mixture of *m*-PhF_2/PhF, which can then be fed into a column of Mg_2(*m*-dobdc) to produce streams of pure PhF and *m*-PhF_2 (SI, Figure S47). As such, the combined use of Mg_2(dobdc) and Mg_2(*m*-dobdc) could potentially enable the atom-economical production of difluorobenzenes via the electrophilic C−H fluorination of fluorobenzene.[61] More broadly, these results confirm that Mg_2(dobdc) and Mg_2(*m*-

https://dx.doi.org/10.1021/jacs.0c11530
J. Am. Chem. Soc. 2021, 143, 1948−1958

dobdc) are matchlessly able to effect the highly challenging separation of fluoroarenes from the corresponding arenes, potentially unlocking new routes to preparing fluoroarenes via C−H fluorination reactions.[14]

Based on these promising results, preliminary experiments were carried out to investigate the ability of Mg_2(dobdc) to purify other fluoroarenes (Figure 10; see also Section 8 of the SI). The fluoroanisole regioisomers (FPhOMe) could be readily separated using Mg_2(dobdc) and were found to exhibit the same trend in adsorption affinity as the difluorobenzenes, namely, *p*-FPhOMe > *m*-FPhOMe > *o*-FPhOMe (SI, Figure S55). This trend is presumed to arise due to bridging Mg···F and Mg···O(Me) interactions between the adjacent metal sites in the framework. In contrast, the selectivity of Mg_2(dobdc) for the fluorotoluenes (FPhMe) followed the trend *m*-FPhMe > *p*-FPhMe > *o*-FPhMe, as confirmed by three-component (SI, Figure S49) and two-component (SI, Figures S50−S52) equilibrium measurements. Notably, this trend is intermediate between that of the difluorobenzenes ($p > m > o$) in Mg_2(dobdc) and that previously reported for the xylenes isomers in Co_2(dobdc) ($o > m > p$).[59] The larger size of methyl groups compared to hydrogen, fluorine, or methoxy groups likely renders *p*-fluorotoluene too long to bridge two metal centers, similar to *p*-xylene,[59] leading to its decreased affinity for Mg_2(dobdc). Finally, Mg_2(dobdc) was found to exhibit slight selectivity for *p*-fluorochlorobenzene (*p*-FPhCl) over *m*-FPhCl, also likely the result of the superior ability of *p*-FPhCl to bridge two magnesium centers. The lower *p*-FPhCl/*m*-FPhCl selectivity (1.3) of Mg_2(dobdc) compared to its *p*-PhF_2/*m*-PhF_2 selectivity (3.1 ± 0.1) is likely due to the decreased hardness of Cl relative to F and the resulting weaker interactions with the magnesium sites. Together, these findings confirm that controlling the interaction of fluoroarenes with two adjacent Mg^{2+} centers in Mg_2(dobdc) and Mg_2(*m*-dobdc) is a powerful general strategy for achieving challenging separations of fluoroarene isomers.

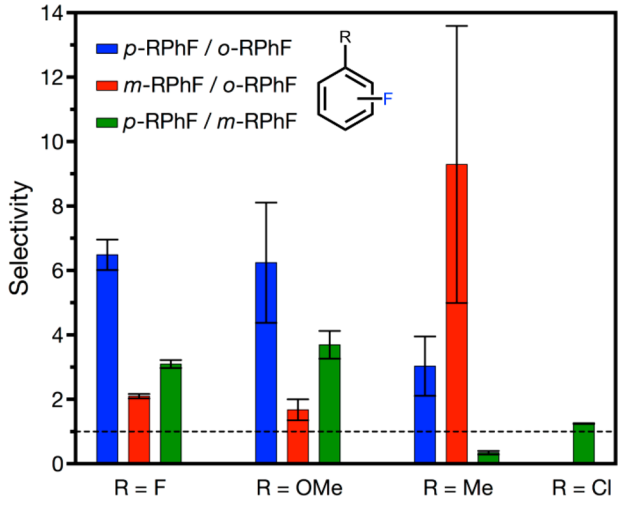

Figure 10. Summary of isothermal equilibrium multicomponent adsorption selectivities of Mg_2(dobdc) for *o*-, *m*-, and *p*-fluoroarenes in heptanes. Samples were dosed with an approximately equimolar mixture (~0.5 M in each aryl fluoride) and allowed to equilibrate at room temperature over 24 h. The data shown are an average of three measurements. The data for the difluorobenzene isomers are included for comparison. A line corresponding to a selectivity of 1 (i.e., not selective) is included for reference.

CONCLUSIONS

The purification of fluoroarene regioisomers is a notoriously challenging separation that hinders the advancement of more direct methods for the production of these critical chemical building blocks. The foregoing computational and experimental results confirm that Mg_2(dobdc) and Mg_2(*m*-dobdc) are uniquely able to separate regioisomeric mixtures of fluoroarenes. These separations are predicated on interactions between fluoroarene isomers and two adjacent framework magnesium sites. In addition, these MOFs enable the separation of fluoroarenes based on the degree of fluorination, which is important for the implementation of new C−H fluorination routes. As such, the separation of larger fluoroarene isomers, such as fluoronaphthalenes and fluorobiphenyls, should be possible using expanded-pore frameworks.[67,89,90] More broadly, the selective interactions of isomeric compounds with multiple strong binding sites within MOFs represents a generalizable strategy for achieving hitherto unrealized liquid-phase separations.

ASSOCIATED CONTENT

Supporting Information

The Supporting Information is available free of charge at https://pubs.acs.org/doi/10.1021/jacs.0c11530.

Experimental details, single-crystal X-ray diffraction structures of Co_2(dobdc)·1.30(*p*-PhF_2) (CCDC 2055904) and Co_2(dobdc)·1.20(*p*-PhF_2) (CCDC 2055905), and all DFT-calculated structures (PDF)

DFT-calculated crystal data for PhF in Mg_2(dobdc) (CIF)

DFT-calculated crystal data for PhF in Mg_2(*m*-dobdc) (CIF)

DFT-calculated crystal data for *p*-PhF_2 in Mg_2(*m*-dobdc) (CIF)

DFT-calculated crystal data for *o*-PhF_2 in Mg_2(*m*-dobdc) (CIF)

DFT-calculated crystal data for *m*-PhF_2 in Mg_2(*m*-dobdc), T-shaped (CIF)

DFT-calculated crystal data for *m*-PhF_2 in Mg_2(dobdc) (CIF)

DFT-calculated crystal data for *o*-PhF_2 in Mg_2(dobdc) (CIF)

DFT-calculated crystal data for *p*-PhF_2 in Mg_2(dobdc) (CIF)

DFT-calculated crystal data for *p*-PhF_2 in Co_2(dobdc) (CIF)

DFT-calculated crystal data for *m*-PhF_2 in Co_2(dobdc) (CIF)

DFT-calculated crystal data for *o*-PhF_2 in Co_2(dobdc) (CIF)

Accession Codes

CCDC 2055904 and 2055905 contain the supplementary crystallographic data for this paper. These data can be obtained free of charge via www.ccdc.cam.ac.uk/data_request/cif, or by emailing data_request@ccdc.cam.ac.uk, or by contacting The Cambridge Crystallographic Data Centre, 12 Union Road, Cambridge CB2 1EZ, UK; fax: +44 1223 336033.

AUTHOR INFORMATION

Corresponding Author

Phillip J. Milner − *Department of Chemistry and Chemical Biology, Cornell University, Ithaca, New York 14850, United*

https://dx.doi.org/10.1021/jacs.0c11530
J. Am. Chem. Soc. 2021, 143, 1948−1958

States; orcid.org/0000-0002-2618-013X;
Email: pjm347@cornell.edu

Authors

Mary E. Zick – *Department of Chemistry and Chemical Biology, Cornell University, Ithaca, New York 14850, United States*

Jung-Hoon Lee – *Computational Science Research Center, Korea Institute of Science and Technology (KIST), Seoul 02792, Republic of Korea;* orcid.org/0000-0002-2983-678X

Miguel I. Gonzalez – *Department of Chemistry, University of California, Berkeley, California 94720, United States*

Ever O. Velasquez – *Department of Chemical and Biomolecular Engineering, University of California, Berkeley, California 94720, United States*

Adam A. Uliana – *Department of Chemical and Biomolecular Engineering, University of California, Berkeley, California 94720, United States*

Jaehwan Kim – *Department of Chemistry and Chemical Biology, Cornell University, Ithaca, New York 14850, United States*

Jeffrey R. Long – *Department of Chemistry, University of California, Berkeley, California 94720, United States; Department of Chemical and Biomolecular Engineering, University of California, Berkeley, California 94720, United States; Materials Sciences Division, Lawrence Berkeley National Laboratory, Berkeley, California 94720, United States;* orcid.org/0000-0002-5324-1321

Complete contact information is available at: https://pubs.acs.org/10.1021/jacs.0c11530

Notes

The authors declare the following competing financial interest(s): P.J.M. and J.R.L. are listed on several patents that included functionalized variants of MOF-74. J.R.L. has a financial interest in and serves on the board of directors of Mosaic Materials, a start-up company working to commercialize metal-organic frameworks for gas separations.

■ ACKNOWLEDGMENTS

We thank the National Institute of General Medical Sciences of the National Institutes of Health for a postdoctoral fellowship for P.J.M. (F32GM120799) to support the initial stages of this work. Further support for this work was provided by the National Institute of General Medical Sciences of the National Institutes of Health under award number R35GM138165 (M.E.Z., J.K., P.J.M.). The content is solely the responsibility of the authors and does not necessarily represent the official views of the National Institutes of Health. Computational work and resources were supported by the KIST Institutional Program (Project No. 2E30460) and KISTI Supercomputing Centre (Project No. KSC-2019-CRE-0149) (J.-H.L.). Crystallographic and breakthrough studies were supported by the U.S. Department of Energy (DOE), Office of Science, Office of Basic Energy Sciences, under Award DE-SC0019992 (M.I.G., E.O.V., A.A.U., J.R.L.). We also thank the National Science Foundation for graduate research fellowships for E.O.V. and A.A.U. This work utilized the resources of the Advanced Light Source at Lawrence Berkeley National Laboratory, a user facility supported by the Director, Office of Science, Office of Basic Energy Sciences, U.S. Department of Energy under Contract No. DE-AC02-05CH11231. This work made use of the Cornell Center for Materials Research Shared Facilities, which are supported through the NSF MRSEC program (DMR-1719875). This work made use of a Bruker INOVA 500 MHz spectrometer, the purchase of which was supported by the National Science Foundation (CHE-1531632). We thank Dr. Katie R. Meihaus (UC Berkeley) for editorial assistance and Dr. Ivan Keresztes (Cornell University) for assistance with solid-state NMR experiments.

■ REFERENCES

(1) Preshlock, S.; Tredwell, M.; Gouverneur, V. ^{18}F-Labeling of Arenes and Heteroarenes for Applications in Positron Emission Tomography. *Chem. Rev.* **2016**, *116* (2), 719–766.

(2) Gillis, E. P.; Eastman, K. J.; Hill, M. D.; Donnelly, D. J.; Meanwell, N. A. Applications of Fluorine in Medicinal Chemistry. *J. Med. Chem.* **2015**, *58* (21), 8315–8359.

(3) Zhou, Y.; Wang, J.; Gu, Z.; Wang, S.; Zhu, W.; Aceña, J. L.; Soloshonok, V. A.; Izawa, K.; Liu, H. Next Generation of Fluorine-Containing Pharmaceuticals, Compounds Currently in Phase II–III Clinical Trials of Major Pharmaceutical Companies: New Structural Trends and Therapeutic Areas. *Chem. Rev.* **2016**, *116* (2), 422–518.

(4) Müller, K.; Faeh, C.; Diederich, F. Fluorine in Pharmaceuticals: Looking Beyond Intuition. *Science* **2007**, *317* (5846), 1881.

(5) Jeschke, P. The Unique Role of Fluorine in the Design of Active Ingredients for Modern Crop Protection. *ChemBioChem* **2004**, *5* (5), 570–589.

(6) Okazoe, T. Overview on the History of Organofluorine Chemistry from the Viewpoint of Material Industry. *Proc. Jpn. Acad., Ser. B* **2009**, *85* (8), 276–289.

(7) Richardson, P. Fluorination Methods for Drug Discovery and Development. *Expert Opin. Drug Discovery* **2016**, *11* (10), 983–999.

(8) Campbell, M. G.; Ritter, T. Modern Carbon–Fluorine Bond Forming Reactions for Aryl Fluoride Synthesis. *Chem. Rev.* **2015**, *115* (2), 612–633.

(9) Champagne, P. A.; Desroches, J.; Hamel, J.-D.; Vandamme, M.; Paquin, J.-F. Monofluorination of Organic Compounds: 10 Years of Innovation. *Chem. Rev.* **2015**, *115* (17), 9073–9174.

(10) Liang, T.; Neumann, C. N.; Ritter, T. Introduction of Fluorine and Fluorine-Containing Functional Groups. *Angew. Chem., Int. Ed.* **2013**, *52* (32), 8214–8264.

(11) Furuya, T.; Klein, J.; Ritter, T. Carbon-Fluorine Bond Formation for the Synthesis of Aryl Fluorides. *Synthesis* **2010**, *2010* (11), 1804–1821.

(12) Balz, G.; Schiemann, G. Über aromatische Fluorverbindungen, I.: Ein neues Verfahren zu ihrer Darstellung. *Ber. Dtsch. Chem. Ges. B* **1927**, *60* (5), 1186–1190.

(13) Park, N. H.; Senter, T. J.; Buchwald, S. L. Rapid Synthesis of Aryl Fluorides in Continuous Flow through the Balz-Schiemann Reaction. *Angew. Chem., Int. Ed.* **2016**, *55* (39), 11907–11911.

(14) Cheng, Q.; Ritter, T. New Directions in C–H Fluorination. *Trends Chem.* **2019**, *1*, 461.

(15) Lin, A.; Huehls, C. B.; Yang, J. Recent Advances in C–H Fluorination. *Org. Chem. Front.* **2014**, *1* (4), 434–438.

(16) Yamamoto, K.; Li, J.; Garber, J. A. O.; Rolfes, J. D.; Boursalian, G. B.; Borghs, J. C.; Genicot, C.; Jacq, J.; van Gastel, M.; Neese, F.; Ritter, T. Palladium-Catalysed Electrophilic Aromatic C–H Fluorination. *Nature* **2018**, *554* (7693), 511–514.

(17) Regalado, E. L.; Makarov, A. A.; McClain, R.; Przybyciel, M.; Welch, C. J. Search for Improved Fluorinated Stationary Phases for Separation of Fluorine-Containing Pharmaceuticals from Their Desfluoro Analogs. *J. Chromatogr. A* **2015**, *1380*, 45–54.

(18) Milner, P. J.; Kinzel, T.; Zhang, Y.; Buchwald, S. L. Studying Regioisomer Formation in the Pd-Catalyzed Fluorination of Aryl Triflates by Deuterium Labeling. *J. Am. Chem. Soc.* **2014**, *136* (44), 15757–15766.

(19) Regalado, E. L.; Zhuang, P.; Chen, Y.; Makarov, A. A.; Schafer, W. A.; McGachy, N.; Welch, C. J. Chromatographic Resolution of Closely Related Species in Pharmaceutical Chemistry: Dehalogenation

Impurities and Mixtures of Halogen Isomers. *Anal. Chem.* **2014**, *86* (1), 805−813.
(20) Lee, H. G.; Milner, P. J.; Buchwald, S. L. Pd-Catalyzed Nucleophilic Fluorination of Aryl Bromides. *J. Am. Chem. Soc.* **2014**, *136* (10), 3792−3795.
(21) Furukawa, H.; Cordova, K. E.; O'Keeffe, M.; Yaghi, O. M. The Chemistry and Applications of Metal-Organic Frameworks. *Science* **2013**, *341* (6149), 1230444−1230444.
(22) Zhang, J.; Chen, J.; Peng, S.; Peng, S.; Zhang, Z.; Tong, Y.; Miller, P. W.; Yan, X.-P. Emerging Porous Materials in Confined Spaces: From Chromatographic Applications to Flow Chemistry. *Chem. Soc. Rev.* **2019**, *48* (9), 2566−2595.
(23) Mukherjee, S.; Desai, A. V.; Ghosh, S. K. Potential of Metal−Organic Frameworks for Adsorptive Separation of Industrially and Environmentally Relevant Liquid Mixtures. *Coord. Chem. Rev.* **2018**, *367*, 82−126.
(24) Wang, X.; Ye, N. Recent Advances in Metal-Organic Frameworks and Covalent Organic Frameworks for Sample Preparation and Chromatographic Analysis. *Electrophoresis* **2017**, *38* (24), 3059−3078.
(25) Zhang, J.; Chen, Z. Metal-Organic Frameworks as Stationary Phase for Application in Chromatographic Separation. *J. Chromatogr. A* **2017**, *1530*, 1−18.
(26) Van de Voorde, B.; Bueken, B.; Denayer, J.; De Vos, D. Adsorptive Separation on Metal−Organic Frameworks in the Liquid Phase. *Chem. Soc. Rev.* **2014**, *43* (16), 5766−5788.
(27) Yusuf, K.; Aqel, A.; ALOthman, Z. Metal-Organic Frameworks in Chromatography. *J. Chromatogr. A* **2014**, *1348*, 1−16.
(28) Yu, Y.; Ren, Y.; Shen, W.; Deng, H.; Gao, Z. Applications of Metal-Organic Frameworks as Stationary Phases in Chromatography. *TrAC, Trends Anal. Chem.* **2013**, *50*, 33−41.
(29) Gu, Z.-Y.; Yang, C.-X.; Chang, N.; Yan, X.-P. Metal−Organic Frameworks for Analytical Chemistry: From Sample Collection to Chromatographic Separation. *Acc. Chem. Res.* **2012**, *45* (5), 734−745.
(30) Li, H.; Wang, K.; Sun, Y.; Lollar, C. T.; Li, J.; Zhou, H.-C. Recent Advances in Gas Storage and Separation Using Metal−Organic Frameworks. *Mater. Today* **2018**, *21* (2), 108−121.
(31) Li, J.-R.; Sculley, J.; Zhou, H.-C. Metal−Organic Frameworks for Separations. *Chem. Rev.* **2012**, *112* (2), 869−932.
(32) Han, S.; Wei, Y.; Valente, C.; Lagzi, I.; Gassensmith, J. J.; Coskun, A.; Stoddart, J. F.; Grzybowski, B. A. Chromatography in a Single Metal−Organic Framework (MOF) Crystal. *J. Am. Chem. Soc.* **2010**, *132* (46), 16358−16361.
(33) Inokuma, Y.; Arai, T.; Fujita, M. Networked Molecular Cages as Crystalline Sponges for Fullerenes and Other Guests. *Nat. Chem.* **2010**, *2* (9), 780−783.
(34) Ahmad, R.; Wong-Foy, A. G.; Matzger, A. J. Microporous Coordination Polymers As Selective Sorbents for Liquid Chromatography. *Langmuir* **2009**, *25* (20), 11977−11979.
(35) Huang, G.; Yang, C.; Xu, Z.; Wu, H.; Li, J.; Zeller, M.; Hunter, A. D.; Chui, S. S.-Y.; Che, C.-M. Shape-Selective Sorption and Fluorescence Sensing of Aromatics in a Flexible Network of Tetrakis[(4-Methylthiophenyl)Ethynyl]Silane and $AgBF_4$. *Chem. Mater.* **2009**, *21* (3), 541−546.
(36) Hasegawa, S.; Horike, S.; Matsuda, R.; Furukawa, S.; Mochizuki, K.; Kinoshita, Y.; Kitagawa, S. Three-Dimensional Porous Coordination Polymer Functionalized with Amide Groups Based on Tridentate Ligand: Selective Sorption and Catalysis. *J. Am. Chem. Soc.* **2007**, *129* (9), 2607−2614.
(37) Kosal, M. E.; Chou, J.-H.; Wilson, S. R.; Suslick, K. S. A Functional Zeolite Analogue Assembled from Metalloporphyrins. *Nat. Mater.* **2002**, *1* (2), 118−121.
(38) Lu, J. Y.; Babb, A. M. An Extremely Stable Open-Framework Metal−Organic Polymer with Expandable Structure and Selective Adsorption Capability. *Chem. Commun.* **2002**, No. 13, 1340−1341.
(39) Yaghi, O. M.; Davis, C. E.; Li, G.; Li, H. Selective Guest Binding by Tailored Channels in a 3-D Porous Zinc(II)−Benzenetricarboxylate Network. *J. Am. Chem. Soc.* **1997**, *119* (12), 2861−2868.
(40) Platero-Prats, A. E.; de la Peña-O'Shea, V. A.; Snejko, N.; Monge, Á.; Gutiérrez-Puebla, E. Dynamic Calcium Metal-Organic Framework Acts as a Selective Organic Solvent Sponge. *Chem. - Eur. J.* **2010**, *16* (38), 11632−11640.
(41) Qiu, L.-G.; Li, Z.-Q.; Wu, Y.; Wang, W.; Xu, T.; Jiang, X. Facile Synthesis of Nanocrystals of a Microporous Metal−Organic Framework by an Ultrasonic Method and Selective Sensing of Organoamines. *Chem. Commun.* **2008**, No. 31, 3642.
(42) Xu, G.; Zhang, X.; Guo, P.; Pan, C.; Zhang, H.; Wang, C. Mn^{II}-Based MIL-53 Analogues: Synthesis Using Neutral Bridging μ_2-Ligands and Application in Liquid-Phase Adsorption and Separation of C6−C8 Aromatics. *J. Am. Chem. Soc.* **2010**, *132* (11), 3656−3657.
(43) Yaghi, O. M.; Li, G.; Li, H. Selective Binding and Removal of Guests in a Microporous Metal−Organic Framework. *Nature* **1995**, *378* (6558), 703−706.
(44) Choi, H. J.; Lee, T. S.; Suh, M. P. Selective Binding of Open Frameworks Assembled from Nickel(II) Macrocyclic Complexes with Organic and Inorganic Guests. *J. Inclusion Phenom. Mol. Recognit. Chem.* **2001**, *41*, 155−162.
(45) Maes, M.; Alaerts, L.; Vermoortele, F.; Ameloot, R.; Couck, S.; Finsy, V.; Denayer, J. F. M.; De Vos, D. E. Separation of C_5-Hydrocarbons on Microporous Materials: Complementary Performance of MOFs and Zeolites. *J. Am. Chem. Soc.* **2010**, *132* (7), 2284−2292.
(46) Maes, M.; Vermoortele, F.; Alaerts, L.; Couck, S.; Kirschhock, C. E. A.; Denayer, J. F. M.; De Vos, D. E. Separation of Styrene and Ethylbenzene on Metal−Organic Frameworks: Analogous Structures with Different Adsorption Mechanisms. *J. Am. Chem. Soc.* **2010**, *132* (43), 15277−15285.
(47) Ameloot, R.; Liekens, A.; Alaerts, L.; Maes, M.; Galarneau, A.; Coq, B.; Desmet, G.; Sels, B. F.; Denayer, J. F. M.; De Vos, D. E. Silica-MOF Composites as a Stationary Phase in Liquid Chromatography. *Eur. J. Inorg. Chem.* **2010**, *2010* (24), 3735−3738.
(48) Kawano, M.; Kawamichi, T.; Haneda, T.; Kojima, T.; Fujita, M. The Modular Synthesis of Functional Porous Coordination Networks. *J. Am. Chem. Soc.* **2007**, *129* (50), 15418−15419.
(49) Hartlieb, K. J.; Holcroft, J. M.; Moghadam, P. Z.; Vermeulen, N. A.; Algaradah, M. M.; Nassar, M. S.; Botros, Y. Y.; Snurr, R. Q.; Stoddart, J. F. CD-MOF: A Versatile Separation Medium. *J. Am. Chem. Soc.* **2016**, *138* (7), 2292−2301.
(50) Maes, M.; Schouteden, S.; Hirai, K.; Furukawa, S.; Kitagawa, S.; De Vos, D. E. Liquid Phase Separation of Polyaromatics on $[Cu_2(BDC)_2(Dabco)]$. *Langmuir* **2011**, *27* (15), 9083−9087.
(51) Liu, Q.-K.; Ma, J.-P.; Dong, Y.-B. Adsorption and Separation of Reactive Aromatic Isomers and Generation and Stabilization of Their Radicals within Cadmium(II)−Triazole Metal−Organic Confined Space in a Single-Crystal-to-Single-Crystal Fashion. *J. Am. Chem. Soc.* **2010**, *132* (20), 7005−7017.
(52) Alaerts, L.; Maes, M.; Giebeler, L.; Jacobs, P. A.; Martens, J. A.; Denayer, J. F. M.; Kirschhock, C. E. A.; De Vos, D. E. Selective Adsorption and Separation of *Ortho*-Substituted Alkylaromatics with the Microporous Aluminum Terephthalate MIL-53. *J. Am. Chem. Soc.* **2008**, *130* (43), 14170−14178.
(53) Alaerts, L.; Kirschhock, C. E. A.; Maes, M.; van der Veen, M. A.; Finsy, V.; Depla, A.; Martens, J. A.; Baron, G. V.; Jacobs, P. A.; Denayer, J. F. M.; De Vos, D. E. Selective Adsorption and Separation of Xylene Isomers and Ethylbenzene with the Microporous Vanadium(IV) Terephthalate MIL-47. *Angew. Chem., Int. Ed.* **2007**, *46* (23), 4293−4297.
(54) Hall, J. N.; Bollini, P. Structure, Characterization, and Catalytic Properties of Open-Metal Sites in Metal Organic Frameworks. *React. Chem. Eng.* **2019**, *4* (2), 207−222.
(55) Pike, S. D.; Crimmin, M. R.; Chaplin, A. B. Organometallic Chemistry Using Partially Fluorinated Benzenes. *Chem. Commun.* **2017**, *53* (26), 3615−3633.
(56) Plenio, H. The Coordination Chemistry of Fluorine in Fluorocarbons. *ChemBioChem* **2004**, *5* (5), 650−655.
(57) Plenio, H. The Coordination Chemistry of the CF Unit in Fluorocarbons. *Chem. Rev.* **1997**, *97* (8), 3363−3384.
(58) Kulawiec, R. J.; Crabtree, R. H. Coordination Chemistry of Halocarbons. *Coord. Chem. Rev.* **1990**, *99*, 89−115.

https://dx.doi.org/10.1021/jacs.0c11530
J. Am. Chem. Soc. 2021, 143, 1948−1958

(59) Gonzalez, M. I.; Kapelewski, M. T.; Bloch, E. D.; Milner, P. J.; Reed, D. A.; Hudson, M. R.; Mason, J. A.; Barin, G.; Brown, C. M.; Long, J. R. Separation of Xylene Isomers through Multiple Metal Site Interactions in Metal−Organic Frameworks. *J. Am. Chem. Soc.* **2018**, *140* (9), 3412−3422.
(60) O'Toole, T. R.; Younathan, J. N.; Sullivan, B. P.; Meyer, T. J. 1,2-Difluorobenzene: A Relatively Inert and Noncoordinating Solvent for Electrochemical Studies on Transition-Metal Complexes. *Inorg. Chem.* **1989**, *28* (20), 3923−3926.
(61) Vasek, A. H.; Sams, L. C. The Reaction of Atomic Fluorine with Fluorobenzene. *J. Fluorine Chem.* **1974**, *3* (3−4), 397−401.
(62) Caskey, S. R.; Wong-Foy, A. G.; Matzger, A. J. Dramatic Tuning of Carbon Dioxide Uptake via Metal Substitution in a Coordination Polymer with Cylindrical Pores. *J. Am. Chem. Soc.* **2008**, *130* (33), 10870−10871.
(63) Dietzel, P. D. C.; Morita, Y.; Blom, R.; Fjellvåg, H. An In Situ High-Temperature Single-Crystal Investigation of a Dehydrated Metal-Organic Framework Compound and Field-Induced Magnetization of One-Dimensional Metal-Oxygen Chains. *Angew. Chem., Int. Ed.* **2005**, *44* (39), 6354−6358.
(64) Rosi, N. L.; Kim, J.; Eddaoudi, M.; Chen, B.; O'Keeffe, M.; Yaghi, O. M. Rod Packings and Metal−Organic Frameworks Constructed from Rod-Shaped Secondary Building Units. *J. Am. Chem. Soc.* **2005**, *127* (5), 1504−1518.
(65) Kapelewski, M. T.; Geier, S. J.; Hudson, M. R.; Stück, D.; Mason, J. A.; Nelson, J. N.; Xiao, D. J.; Hulvey, Z.; Gilmour, E.; FitzGerald, S. A.; Head-Gordon, M.; Brown, C. M.; Long, J. R. M_2(*m*-dobdc) (M = Mg, Mn, Fe, Co, Ni) Metal−Organic Frameworks Exhibiting Increased Charge Density and Enhanced H_2 Binding at the Open Metal Sites. *J. Am. Chem. Soc.* **2014**, *136* (34), 12119−12129.
(66) McDonald, T. M.; Mason, J. A.; Kong, X.; Bloch, E. D.; Gygi, D.; Dani, A.; Crocellà, V.; Giordanino, F.; Odoh, S. O.; Drisdell, W. S.; Vlaisavljevich, B.; Dzubak, A. L.; Poloni, R.; Schnell, S. K.; Planas, N.; Lee, K.; Pascal, T.; Wan, L. F.; Prendergast, D.; Neaton, J. B.; Smit, B.; Kortright, J. B.; Gagliardi, L.; Bordiga, S.; Reimer, J. A.; Long, J. R. Cooperative Insertion of CO_2 in Diamine-Appended Metal-Organic Frameworks. *Nature* **2015**, *519* (7543), 303−308.
(67) McDonald, T. M.; Lee, W. R.; Mason, J. A.; Wiers, B. M.; Hong, C. S.; Long, J. R. Capture of Carbon Dioxide from Air and Flue Gas in the Alkylamine-Appended Metal−Organic Framework Mmen-Mg_2(dobpdc). *J. Am. Chem. Soc.* **2012**, *134* (16), 7056−7065.
(68) Siegelman, R. L.; McDonald, T. M.; Gonzalez, M. I.; Martell, J. D.; Milner, P. J.; Mason, J. A.; Berger, A. H.; Bhown, A. S.; Long, J. R. Controlling Cooperative CO_2 Adsorption in Diamine-Appended Mg_2(dobpdc) Metal−Organic Frameworks. *J. Am. Chem. Soc.* **2017**, *139* (30), 10526−10538.
(69) Chui, S. S. A Chemically Functionalizable Nanoporous Material $[Cu_3(TMA)_2(H_2O)_3]$n. *Science* **1999**, *283* (5405), 1148−1150.
(70) Smaldone, R. A.; Forgan, R. S.; Furukawa, H.; Gassensmith, J. J.; Slawin, A. M. Z.; Yaghi, O. M.; Stoddart, J. F. Metal-Organic Frameworks from Edible Natural Products. *Angew. Chem., Int. Ed.* **2010**, *49* (46), 8630−8634.
(71) Parr, R. G.; Pearson, R. G. Absolute Hardness: Companion Parameter to Absolute Electronegativity. *J. Am. Chem. Soc.* **1983**, *105* (26), 7512−7516.
(72) Pahl, J.; Stennett, T. E.; Volland, M.; Guldi, D. M.; Harder, S. Complexation and Versatile Reactivity of a Highly Lewis Acidic Cationic Mg Complex with Alkynes and Phosphines. *Chem. - Eur. J.* **2019**, *25* (8), 2025−2034.
(73) Pahl, J.; Brand, S.; Elsen, H.; Harder, S. Highly Lewis Acidic Cationic Alkaline Earth Metal Complexes. *Chem. Commun.* **2018**, *54* (63), 8685−8688.
(74) Gonzalez, M. I.; Mason, J. A.; Bloch, E. D.; Teat, S. J.; Gagnon, K. J.; Morrison, G. Y.; Queen, W. L.; Long, J. R. Structural Characterization of Framework−Gas Interactions in the Metal−Organic Framework Co_2(dobdc) by in Situ Single-Crystal X-Ray Diffraction. *Chem. Sci.* **2017**, *8* (6), 4387−4398.
(75) Bouwkamp, M. W.; Budzelaar, P. H. M.; Gercama, J.; Del Hierro Morales, I.; de Wolf, J.; Meetsma, A.; Troyanov, S. I.; Teuben, J. H.; Hessen, B. Naked $(C_5Me_5)_2$ M Cations (M = Sc, Ti, and V) and Their Fluoroarene Complexes. *J. Am. Chem. Soc.* **2005**, *127* (41), 14310−14319.
(76) Basuli, F.; Aneetha, H.; Huffman, J. C.; Mindiola, D. J. A Fluorobenzene Adduct of Ti(IV), and Catalytic Carboamination to Prepare α,β-Unsaturated Imines and Triaryl-Substituted Quinolines. *J. Am. Chem. Soc.* **2005**, *127* (51), 17992−17993.
(77) Bouwkamp, M. W.; de Wolf, J.; del Hierro Morales, I.; Gercama, J.; Meetsma, A.; Troyanov, S. I.; Hessen, B.; Teuben, J. H. Structure of the Decamethyl Titanocene Cation, a Metallocene with Two Agostic C−H Bonds, and Its Interaction with Fluorocarbons. *J. Am. Chem. Soc.* **2002**, *124* (44), 12956−12957.
(78) Birnbaum, E. R.; Hodge, J. A.; Grinstaff, M. W.; Schaefer, W. P.; Henling, L.; Labinger, J. A.; Bercaw, J. E.; Gray, H. B. ^{19}F NMR Spectra and Structures of Halogenated Porphyrins. *Inorg. Chem.* **1995**, *34* (14), 3625−3632.
(79) Thompson, J. S.; Sorrell, T.; Marks, T. J.; Ibers, J. A. Synthesis, Structure, and Spectroscopy of Pseudotetrahedral $Co^{II}N_3$(SR) Complexes. Active Site Approximations to the Cobalt(II)-Substituted Type 1 Copper Proteins. *J. Am. Chem. Soc.* **1979**, *101* (15), 4193−4200.
(80) Eisenstein, O.; Milani, J.; Perutz, R. N. Selectivity of C−H Activation and Competition between C−H and C−F Bond Activation at Fluorocarbons. *Chem. Rev.* **2017**, *117* (13), 8710−8753.
(81) Ahrens, T.; Kohlmann, J.; Ahrens, M.; Braun, T. Functionalization of Fluorinated Molecules by Transition-Metal-Mediated C−F Bond Activation To Access Fluorinated Building Blocks. *Chem. Rev.* **2015**, *115* (2), 931−972.
(82) Amii, H.; Uneyama, K. C−F Bond Activation in Organic Synthesis. *Chem. Rev.* **2009**, *109* (5), 2119−2183.
(83) Boyd, T. M.; Tegner, B. E.; Tizzard, G. J.; Martínez-Martínez, A. J.; Neale, S. E.; Hayward, M. A.; Coles, S. J.; Macgregor, S. A.; Weller, A. S. A Structurally Characterized Cobalt(I) $\sum$-Alkane Complex. *Angew. Chem., Int. Ed.* **2020**, *59* (15), 6177−6181.
(84) Zhong, H.; Friedfeld, M. R.; Chirik, P. J. Syntheses and Catalytic Hydrogenation Performance of Cationic Bis(Phosphine) Cobalt(I) Diene and Arene Compounds. *Angew. Chem., Int. Ed.* **2019**, *58* (27), 9194−9198.
(85) Meier, S. C.; Himmel, D.; Krossing, I. How Does the Environment Influence a Given Cation? A Systematic Investigation of $[Co(CO)_5]^+$ in Gas Phase, Solution, and Solid State. *Chem. - Eur. J.* **2018**, *24* (72), 19348−19360.
(86) Meier, S. C.; Holz, A.; Kulenkampff, J.; Schmidt, A.; Kratzert, D.; Himmel, D.; Schmitz, D.; Scheidt, E.-W.; Scherer, W.; Bülow, C.; Timm, M.; Lindblad, R.; Akin, S. T.; Zamudio-Bayer, V.; von Issendorff, B.; Duncan, M. A.; Lau, J. T.; Krossing, I. Access to the Bis-Benzene Cobalt(I) Sandwich Cation and Its Derivatives: Synthons for a "Naked" Cobalt(I) Source? *Angew. Chem., Int. Ed.* **2018**, *57* (30), 9310−9314.
(87) Meier, S. C.; Holz, A.; Schmidt, A.; Kratzert, D.; Himmel, D.; Krossing, I. From an Easily Accessible Pentacarbonylcobalt(I) Salt to Piano-Stool Cations $[(Arene)Co(CO)_2]^+$. *Chem. - Eur. J.* **2017**, *23* (58), 14658−14664.
(88) Lei, H.; Fettinger, J. C.; Power, P. P. Reduction of Terphenyl Co(II) Halide Derivatives in the Presence of Arenes: Insertion of Co(I) into a C−F Bond. *Inorg. Chem.* **2012**, *51* (3), 1821−1826.
(89) Deng, H.; Grunder, S.; Cordova, K. E.; Valente, C.; Furukawa, H.; Hmadeh, M.; Gandara, F.; Whalley, A. C.; Liu, Z.; Asahina, S.; Kazumori, H.; O'Keeffe, M.; Terasaki, O.; Stoddart, J. F.; Yaghi, O. M. Large-Pore Apertures in a Series of Metal-Organic Frameworks. *Science* **2012**, *336* (6084), 1018−1023.
(90) Milner, P. J.; Martell, J. D.; Siegelman, R. L.; Gygi, D.; Weston, S. C.; Long, J. R. Overcoming Double-Step CO_2 Adsorption and Minimizing Water Co-Adsorption in Bulky Diamine-Appended Variants of Mg_2(dobpdc). *Chem. Sci.* **2018**, *9* (1), 160−174.

https://dx.doi.org/10.1021/jacs.0c11530
J. Am. Chem. Soc. 2021, 143, 1948−1958